Crystal Structure of Bitiscetin, a von Willebrand Factor-Dependent Platelet Aggregation Inducer[†,‡]

Shoko Hirotsu,[§] Hiroshi Mizuno,*[,§] Kouichi Fukuda,[§] Ma Chun Qi,[||] Taei Matsui,[⊥] Jiharu Hamako,[⊥] Takashi Morita,[||] and Koiti Titani[⊥]

Department of Biochemistry, National Institute of Agrobiological Sciences, Tsukuba, Ibaraki 305-8602, Japan, Department of Biochemistry, Meiji Pharmaceutical University, Kiyose, Tokyo 204-8588, Japan, and Division of Biomedical Polymer Science, Institute for Comprehensive Medical Science, Fujita Health University, Toyoake, Aichi 470-1192, Japan

Received July 17, 2001; Revised Manuscript Received September 12, 2001

ABSTRACT: Bitiscetin, a C-type lectin-like protein isolated from the venom of the snake *Bitis arientans*, promotes the interactions between plasma von Willebrand factor (VWF) and platelet membrane glycoprotein Ib (GPIb) to induce platelet aggregation. We report here the crystal structure of bitiscetin at 2.0 Å resolution. The overall fold is similar to those of coagulation factor IX/X-binding protein (IX/X-bp) and flavocetin-A (a GPIb-binding protein), although these three proteins are functionally distinct from one another. The characteristic property determining target recognition is explained mainly by the differences in the surface potential on the central concave surface. A negatively charged patch on the surface of bitiscetin is a candidate for the site of binding to the positively charged surface of the VWF A1 domain, as shown in the case of another platelet aggregation inducer, botrocetin. However, a positively charged patch near the central concave surface is unique for bitiscetin and suggests that it is the binding site for the negatively charged surface of the VWF A3 domain. Thus, the interactions accounting for VWF activation by bitiscetin possibly involve both the A1 and A3 domains of VWF, indicating a specific mechanism of VWF activation by bitiscetin.

Bitiscetin, a protein isolated from the venom of the snake *Bitis arientans*, promotes interactions between plasma von Willebrand factor (VWF)[1] and platelet membrane glycoprotein Ib (GPIb) to induce platelet aggregation (*1*). VWF is a disulfide-linked multimeric protein composed of identical 275 kDa subunits and mediates the adhesion of platelets to the injured vessel walls by binding both GPIb and subendotheliums exposed on the injured vessel wall, which is the first step in the formation of a platelet plug in hemostasis (*2*). It is known that some conformational changes in the structure of VWF are necessary for the binding of VWF to GPIb, and it is likely that in vivo those conformational changes are achieved by its binding to exposed subendotheliums, particularly under conditions of high shear stress (*3*−*5*). Because of the difficulties of investigating such an in vivo activation mechanism of VWF, especially at the atomic level, nonphysiological activators seem to be very important as a tool for elucidating the activation mechanism of VWF. Bitiscetin described above and botrocetin isolated from the venom of *Bothrops jararaca* (*6*) are such VWF activator proteins. They bind directly to VWF in vitro to form an active complex, and platelet aggregation is induced via interactions between the active complex and GPIb (*1*, *7*, *8*). Bitiscetin, as well as botrocetin, belongs to the C-type lectin superfamily, but it is a heterodimer composed of homologous α- and β-subunits. Each subunit possesses within its structure the carbohydrate recognition domain of C-type lectin, and hereafter, these proteins are termed C-type lectin-like proteins. Up to now, a number of these proteins have been isolated from snake venoms. The amino acid sequence of these proteins was first determined for factor IX/factor X-binding protein (IX/X-bp) from the venom of habu snake (*Trimeresurus flavoviridis*) (*9*), and the first crystal structure analysis (*10*) was also carried out using IX/X-bp. In this crystal structure, the molecule was found to be dimerized by domain swapping, generating a central concave surface that is important as a binding site for the target molecule. Indeed, the recently determined crystal structure of the complex between X-bp and the Gla (γ-carboxyglutamic acid) domain of factor X demonstrated that the concave surface is the actual binding site for the Gla domain (*11*). The crystal structure of botrocetin (*12*) also showed that a negatively charged patch on the concave surface is a candidate site for binding to a positively charged surface of the VWF A1 domain. This

[†] This work was supported in part by Special Coordination Funds for the Promotion of Science and Technology of STA to H.M., by a Research Grant for Cardiovascular Diseases (8A-1) from the Ministry of Health and Welfare to T. Morita, and by Grants-in-Aid from the Ministry of Education, Culture and Science to T. Morita and K.T.

[‡] The atomic coordinates have been deposited in the Protein Data Bank as entry 1JWI.

* To whom correspondence should be addressed: Department of Biochemistry, National Institute of Agrobiological Sciences, Tsukuba, Ibaraki 305-8602, Japan. Telephone: +81-298-38-7014. Fax: +81-298-38-7408. E-mail: mizuno@affrc.go.jp.

[§] National Institute of Agrobiological Sciences.

[||] Meiji Pharmaceutical University.

[⊥] Fujita Health University.

[1] Abbreviations: VWF, von Willebrand factor; CRD, carbohydrate recognition domain; GP, glycoprotein; FL-A, flavocetin-A; IX/X-bp, coagulation factors IX/X-binding protein; IX-bp, coagulation factor IX-binding protein; X-bp, coagulation factor X-binding protein; PEG, polyethylene glycol; Tris, 2-amino-2-(hydroxymethyl)-1,3-propanediol.

10.1021/bi0114933 CCC: $20.00
Published on Web 10/16/2001

structural feature is consistent with some biochemical data showing botrocetin binding to the A1 domain alone (*13*). On the other hand, bitiscetin was reported to bind to the VWF A3 domain, with the possibility that it might bind to the A1 domain concomitantly (*14*). A number of biochemical experiments have revealed that both the A1 and A3 domains of VWF are essential for biological function; that is, the former mediates the binding to GPIb, and the latter the binding to type I or type III collagen, the constituent subendotheliums. It would be of further interest if bitiscetin were to bind to the VWF A3 domain, because it would lend weight to the hypothesis that the activity of the platelet-binding domain (VWF A1) can be regulated by a subendothelium-binding domain (VWF A3) (*14*). One of the major differences between bitiscetin and botrocetin is in the electrostatic nature of their molecular surfaces. Bitiscetin is charged positively with a pI of 9.1, whereas botrocetin is charged negatively with a pI of 4.6 (*1*). This may be related to a difference in the manner in which the two proteins interact with their targets. To further understand the activation mechanism of VWF by bitiscetin, we have crystallized bitiscetin and determined its structure at 2.0 Å resolution.

MATERIALS AND METHODS

Protein Preparation, Crystallization, and Data Collection. Bitiscetin was purified from *B. arietans* venom by the method previously described (*1*). For crystallization, the purified protein was concentrated to ~5 mg/mL in 50 mM Tris-HCl buffer (pH 8.5) containing 100 mM NaCl. Crystals suitable for X-ray structural analysis were grown over a period of 2 weeks at 20 °C by the hanging-drop vapor-diffusion method by mixing 1 μL of the protein solution and the same volume of a reservoir solution containing 100 mM Tris-HCl (pH 8.5), 10% polyethylene glycol (PEG3350 or PEG6000), and 100 mM $CaCl_2$. The crystals belonged to orthorhombic space group $P2_12_12_1$ and contained one dimer per asymmetric unit with the following unit cell dimensions: $a = 35.4$ Å, $b = 60.9$ Å, $c = 122.2$ Å. Data were collected to 2.0 Å resolution at room temperature with an R-AXIS IV imaging-plate area detector (Rigaku, Tokyo, Japan) with a crystal-to-detector distance of 150 mm using Cu Kα radiation generated by a rotating anode generator (Rigaku Ultra-X). All diffraction data were processed by DENZO and scaled by SCALEPACK (*15*).

Phasing and Refinement. Initial phases for the electron density map were calculated using the 2.5 Å resolution data by the molecular replacement (MR) method using the program AmoRe from the CCP4 suites (*16*). The polyalanine model of factor IX-binding protein (IX-bp) (PDB entry 1BJ3) was used for the rotation and translation searches. The searches were performed with the data in a range of 12−5 Å resolution to produce a solution with a correlation coefficient of 0.42 and an *R*-value of 0.52. The rigid body refinement using AMoRe led to a model with a correlation coefficient of 0.44 and an *R*-value of 0.48. Although the initial electron density of the side chains of bitiscetin was poor, it gradually improved as the iterative refinements of the model were performed. The model was successfully refined to an *R*-factor of 0.32 and an R_{free} of 0.39 by simulated annealing with a torsion angle using the program CNS (*17*). Further refinements were performed with several cycles of Cartesian simulated annealing refinement, individual *B*-factor refinement, and manual model rebuilding using the program QUANTA (Molecular Simulations, Inc., Waltham, MA) until the R_{free} dropped to <0.30. Water molecules were located by peak searches in CNS. All peaks were inspected manually and assigned as water if the density was >1σ in a $2F_o - F_c$ map, there were appropriate distances (2.6−4.0 Å) from protein atoms, and the *B*-factor was less than 50 Å^2. The final cycles of refinement were performed using the diffraction data to 2.0 Å resolution, which yielded an *R*-factor of 0.207 and an R_{free} of 0.252. Throughout the model building and refinement process, 10% of the reflec-

Table 1: Statistics of Data Collection and Structure Refinement

data collection	
resolution range (Å)	65−2.0 (2.09−2.0)[a]
total no. of reflections	566351
no. of unique reflections	18662
mosaicity (deg)	0.4
I/σ	18.9 (4.3)
completeness	98.8 (96.9)
R_{sym} (%)	9.3 (26.4)
structure refinement	
resolution range (Å)	8.0−2.0
no. of non-hydrogen protein atoms	2005
no. of water molecules	143
R-factor[b]	0.207
R_{free}[c]	0.252
mean *B*-values (Å^2)	24.2
rms deviations from ideal geometry	
bond lengths (Å)	0.06
bond angles (deg)	1.3

[a] Numbers in parentheses refer to the values for the outer shell. [b] *R*-factor = $\sum||F_{obs}| - |F_{calc}||/\sum|F_{obs}|$. [c] R_{free} was calculated with a randomly selected 10% of the reflections not used in the refinement.

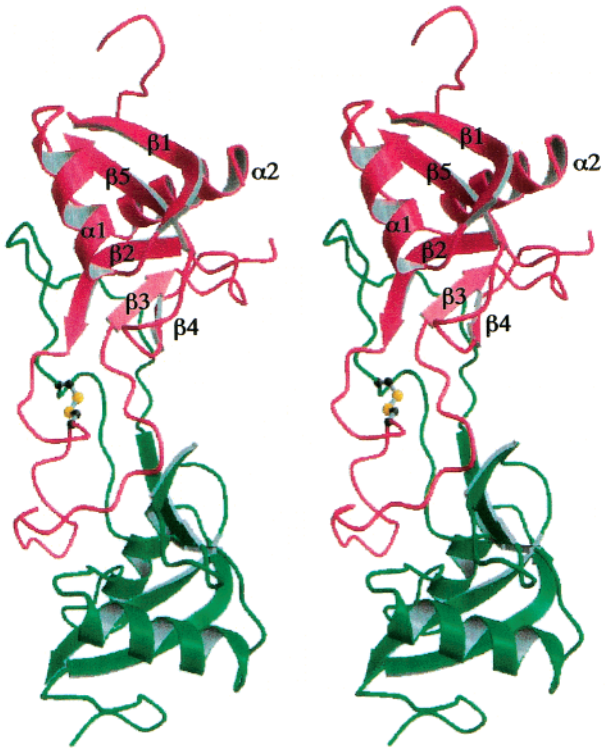

FIGURE 1: Stereoview of the overall structure of bitiscetin. The elements of the α-subunit are shown in magenta and those of the *β*-subunit in green. The side chains of two cysteine residues (Cys 79 of the α-subunit and Cys 77 of the *β*-subunit) forming an interchain disulfide bond are shown by means of a ball-and-stick model.

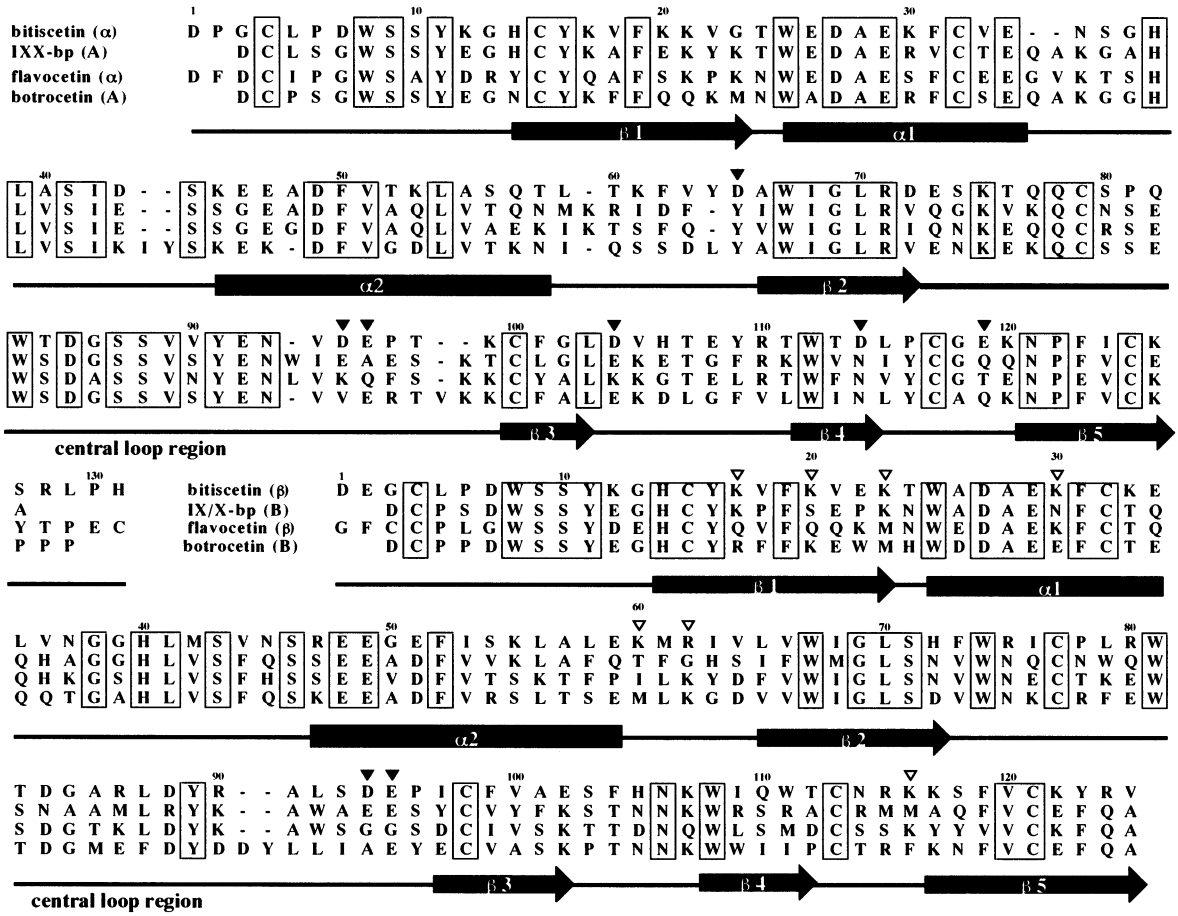

FIGURE 2: Sequence alignment of bitiscetin with other C-type lectin-like proteins. The residues forming an acidic patch on the concave surface of bitiscetin are denoted by solid triangles above the alignment, and residues making up a basic patch near the concave surface of bitiscetin are denoted by open triangles. The secondary structural elements are shown by arrows for β-sheets and rectangles for α-helices.

tions were excluded to monitor R_{free}. Bulk solvent correction was also applied during the refinement. The current model includes 244 of 256 residues of bitiscetin, together with 143 water molecules. Residues 1−3, 60, 61, and 128−131 in the α-subunit and residues 1 and 2 in the β-subunit were not included in the model because of their poor electron density. All residues in the model were in the most favorable region (92.2%) or in the additional allowed region (7.8%) of the Ramachandran plot defined by PROCHECK (*18*). Ribbon models of the main chain fold of the protein were drawn by using the programs MOLSCRIPT (*19*) and QUANTA (Molecular Simulations, Inc.), and the surface representation of the protein was drawn using the program GRASP (*20*). The statistics of data collection and refinement are listed in Table 1.

RESULTS AND DISCUSSION

Overall Structure. The homologous α- and β-subunits of bitiscetin were related by a pseudodyad which was perpendicular to the long axis of the molecule (Figure 1), forming a domain-swapped heterodimer. The conventional carbohydrate binding site of C-type lectin was disrupted by this domain swapping as previously described in structures of IX/X-bp (*10*) and IX-bp (*22*). This is the reason C-type lectin-like proteins have no lectin activity. The main chain fold of bitiscetin was similar to those of homologous C-type lectin-like proteins with known structures, as might be expected because of their high degree of sequence homology (*21*) (Figure 2). However, bitiscetin did not show evidence of being able to bind to Ca^{2+} ions, as in the case of IX/X-bp (*10*) and IX-bp (*22*). In the conventional Ca^{2+}-binding site, amino acid residues used for Ca^{2+} binding were replaced with other amino acids as will be discussed later. Residues 61 and 62 in the loop region between helix α2 and strand β2 of the α-subunit and the N- and C-terminal regions appeared to be obscured by disorder. Each subunit of bitiscetin was comprised of a globular unit and a central loop. Each central loop was extended into the globular unit of the adjoining subunit, resulting in three-dimensional domain swapping (*23*) as previously described in the cases of IX/X-bp and IX-bp (*10*, *22*). This dimer was stabilized by an interchain disulfide bond between Cys 79α and Cys 77β as well as by domain swapping. This type of dimerization generates a unique central concave surface (on the right side of the molecule, as seen in Figure 1), which is important as a binding site for the target molecule and expression of function (see below).

Comparison of the Structures of Bitiscetin and Other Functionally Distinct C-Type Lectin-like Proteins. As previously mentioned, bitiscetin is very similar to other C-type lectin-like proteins in both amino acid sequence and main chain fold. The α- and β-subunits of bitiscetin are approximately 49 and 42% identical in pairwise sequence to the corresponding subunit of IX/X-bp, respectively, and 48 and 42% to that of IX-bp, 41 and 41% to that of X-bp from *Deinagkistrodon acutus* (*24*), 48 and 42% to that of

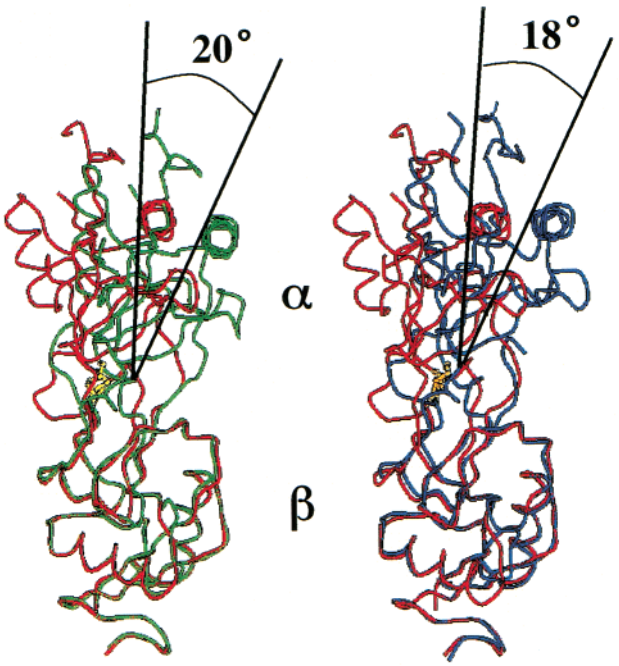

FIGURE 3: Superpositions of the globular units of the β-subunits of bitiscetin (red) and IX/X-bp (green) on the left and of bitiscetin (red) and botrocetin (blue) on the right.

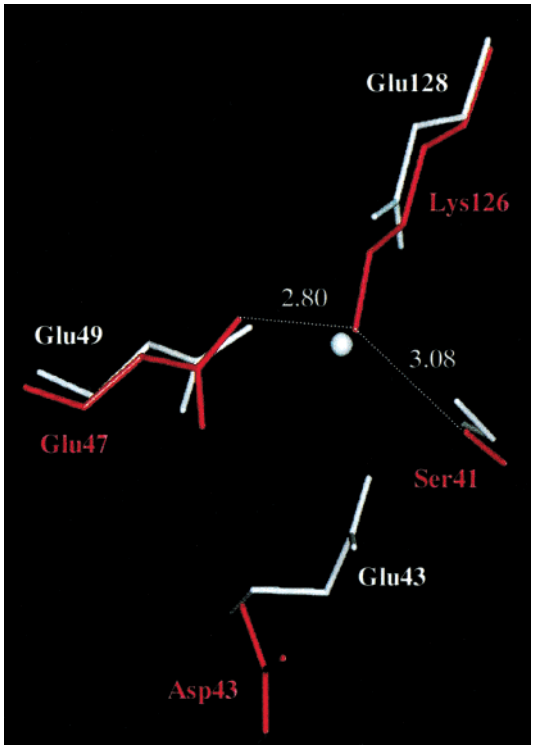

FIGURE 4: Superposition of Ca^{2+}-binding sites in the α-subunit of IX/X-bp (white) and the corresponding region of bitiscetin (red). Ca^{2+} in IX/X-bp is shown as a white sphere.

flavocetin-A (FL-A) from *T. flavoviridis* (*25*), and 50 and 45% to that of botrocetin, respectively. The backbone chain of each subunit of bitiscetin superimposes well with those of other proteins. Average rms differences for equivalent α-carbon atoms of the α- and β-subunit (except for the central loop region) of bitiscetin were 1.30 and 0.94 Å over IX/X-bp, 1.22 and 1.05 Å over IX-bp, 1.35 and 1.00 Å over X-bp in the complex with the Gla domain (*11*), 1.30 and 1.15 Å over FL-A (*26*), and 1.37 and 1.92 Å over botrocetin (*12*), respectively. If the central loop or the adjoining subunit was added for the superposition calculation, the rms difference values increased markedly. This was because the relative orientation of the two subunits was different between the two proteins, as was pointed out previously in the comparison between IX/X-bp and IX-bp (*22*). Figure 3 shows a typical difference; that is, when the β-subunits of bitiscetin and IX/X-bp are superimposed, a 20° rotation of the α-subunit of bitiscetin around the axis, which passes in the proximity of the interchain disulfide bond, is required for the superposition of the corresponding subunit of IX/X-bp. Similarly, an 18° rotation of the α-subunit of bitiscetin is required when compared with botrocetin. These values are exceptionally large because the corresponding value was ≤6° when compared between any two IX/X-bp, IX-bp, and X-bp species. It is likely that the large difference observed in bitiscetin is based not only on hingelike motions but also on structural changes in the central loop. When only the central loop of the α- and β-subunits of bitiscetin and the corresponding subunit of IX/X-bp are superimposed, the rmsd is 0.54 and 0.87 Å for 15 and 17 equivalent α-carbon atoms in the center of the loop, respectively, and 2.03 and 3.08 Å for the remaining 11 and 7 α-carbon atoms in the N- and C-terminal regions, respectively. The larger displacements at the bases of each loop may largely be attributed to the four Pro residues in that region, which affect the orientation of each loop, that is, the relative orientation of the two subunits of bitiscetin. It is apparent therefore that the former corresponds to dynamic behavior between the two subunits, which is analogous to domain movements proposed by Gernstein et al. (*27*), while the latter is sequence-dependent and not dynamic.

Bitiscetin contained no bound Ca^{2+} ions, although it was crystallized in the presence of 10 mM $CaCl_2$. In the α-subunit, the two glutamic acids, conserved for coordination to Ca^{2+} in a conventional Ca^{2+}-binding site, were replaced with Asp 43 and Lys 126. The Nζ atom of Lys 130 was close to the position corresponding to the Ca^{2+} occupied in IX/X-bp, and contributed to the neutralization of negative charges and to the stabilization via hydrogen bonding to the Oϵ atom of Glu 47A (2.80 Å) and the Oγ atom of Ser 41A (3.08 Å) (Figure 4). The side chain of Asp 43 was flipped out and exposed to the solvent, causing it to interact with a water molecule. A similar structure was also observed in the corresponding site in the β-subunit.

Comparison of the Surface Potentials of Bitiscetin and Other C-Type Lectin-like Proteins. C-Type lectin-like proteins from snake venoms have the distinct ability to recognize different target molecules (*28*), although their main chain folds are very similar to one another. This functional difference may originate from the structure and surface potentials around the binding site for the target molecule. The coagulation factor-binding proteins (IX/X-bp, IX-bp, and X-bp) have a positively charged patch conserved on the central concave surface. Figure 5 shows surface potential representations of C-type lectin-like proteins designed for recognizing different target molecules. They appear to differ especially on the concave surface. FL-A has two hydrophilic patches which form a putative binding site on the concave surface for GPIb (*26*). Different surface potentials reflect the composition of amino acid residues making up the central

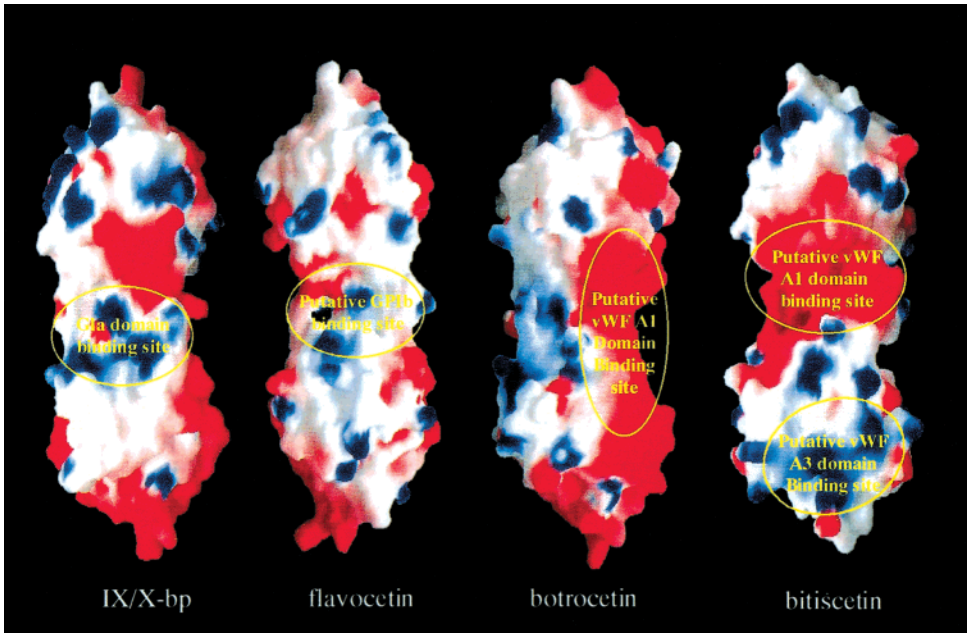

FIGURE 5: Surface representations of IX/X-bp, flavocetin (FL-A), botrocetin, and bitiscetin. Blue corresponds to positive and red to negative potentials. Upper and lower halves of each molecule correspond to α(A)- and *β*(B)-subunits, respectively. The proteins have charge distributions that are different from one another, particularly on the central concave surface used for binding, as indicated.

concave surface. Typical examples are the Arg residues (Arg 107, Arg 109, and Arg 112) of the B-subunit of IX/X-bp replaced with noncharged residues in bitiscetin (Ile 109, Trp 111, and Asn 114) and FL-A (Leu 109, Met 111, and Ser 114) (Figure 2). Of the eight acidic residues of bitiscetin, four residues (Asp 65α, Glu 96α, Asp 114α, and Glu 119α) are replaced with noncharged residues in IX/X-bp (Tyr 65, Ala 97, Asn 116, and Gln 121), and all eight residues are replaced with nonacidic residues in FL-A (Tyr 67, Lys 98, Glu 99, Lys 108, Asn 118, Thr 123, Gly 94*β*, and Gly 95*β*). In bitiscetin, a number of acidic residues (Figure 2) are concentrated in the concave surface, forming an extensive acidic surface (Figure 5), which resembles the surface potentials of botrocetin, a candidate for binding to a positively charged surface of the VWF A1 domain containing helix α6 and the N-terminal portion of helix α5 (*29*).

Implication for Target Binding. The site of binding of VWF to botrocetin was recently assigned to residues Arg 629, Arg 632, Arg 636, and Lys 667 in the A1 domain using charged-to-alanine scanning mutagenesis (*30*, *31*). The crystal structure of botrocetin, on the other hand, showed that the negatively charged patch on the central concave surface is a putative binding site for the positively charged patch containing the basic residues listed above. The results of this study suggest that a negatively charged patch in the central concave surface of bitiscetin resembles somewhat that of botrocetin, and binds to the VWF A1 domain overlapping the botrocetin binding site. This is consistent with the results of charged-to-alanine scanning mutagenesis of the VWF A1 domain of bitiscetin which is similar to that of botrocetin (*32*). However, the charge distributions in these two proteins, except for the concave surfaces, are quite different. Bitiscetin has a basic surface as a whole, while botrocetin has a rather acidic surface, reflecting their pI values (9.1 for bitiscetin and 4.6 for botrocetin). Bitiscetin had solvent accessible basic residues consisting of Lys 17, Lys 20, Lys 23, Lys 30, Lys 60, Arg 62, and Lys 116 which were concentrated on the *β*-subunit and formed a unique positively charged patch

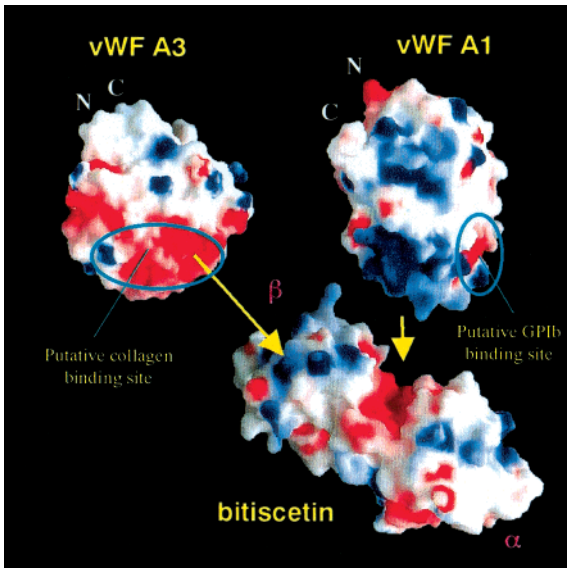

FIGURE 6: Surface representations of bitiscetin, the VWF A1 and A3 domains, and their putative binding sites. Arrows denote the possible docking directions of the VWF A1 and A3 domains with their complementary charged surfaces on bitiscetin. Letters N and C show the N- and C-termini of each domain.

(Figure 5). This patch is another candidate for binding to a negatively charged patch of the VWF A3 domain (*33*), because these interactions explain the results of recent biochemical experiments in which bitiscetin was found to bind to an acidic region of the VWF A3 domain (*14*). Consequently, bitiscetin may bind to both the VWF A1 and VWF A3 domains. The former binding site is similar to that of botrocetin, but the latter is uniquely different. Figure 6 shows a model in which the VWF A1 and VWF A3 domains approach and bind to complementary charged patches on bitiscetin. This docking model is of particular relevance because (1) the C-terminal residue of the VWF A1 domain (Thr 705) and the N-terminal residue of the VWF A3 domain (Gln 925) are spatially close enough together to allow the

VWF A2 domain, which may take on a cuboid structure similar to the VWF A1 or VWF A3 domain (the N- and C-termini are spatialy close together), to be fitted into and connected to the neighboring domains and (2) the putative collagen binding site located on the acidic surface of the VWF A3 domain is the appropriate distance from the putative GPIb binding site on the VWF A1 domain. Thus, the crystal structure of bitiscetin presented here appears to provide relevant insight into the possible interacting surfaces in both bitiscetin and VWF during VWF activation by bitiscetin. Further investigations, including structural analysis of the complex, together with additional biochemical data, should lead to a clear understanding of the mechanism of bitiscetin-related VWF activation.

REFERENCES

1. Hamako, J., Matsui, T., Suzuki, M., Ito, M., Makita, K., Fujimura, Y., Ozeki, Y., and Titani, K. (1996) *Biochem. Biophys. Res. Commun. 226*, 273−279.
2. Wagner, D. D. (1990) *Annu. Rev. Cell Biol. 6*, 217−246.
3. Goto, S., Salomon, D. R., Ikeda, Y., and Ruggeri, Z. M. (1995) *J. Biol. Chem. 279*, 23352−23361.
4. Siedlecki, C. A., Lestini, B. J., Kottke-Marchant, K., Eppell, S. J., Wilson, D. L., and Marchant, R. E. (1996) *Blood 88*, 2939−2950.
5. Miyata, S., Goto, S., Federici, A. B., Ware, J., and Ruggeri, Z. M. (1996) *J. Biol. Chem. 271*, 9046−9053.
6. Read, M. S., Smith, S. V., Lamb, M. A., and Brinkhous, K. M. (1989) *Blood 74*, 1031−1035.
7. Fujimura, Y., Holland, L. Z., and Zimmerman, T. S. (1987) *Blood 70*, 985−988.
8. Andrews, R. K., Booth, W. J., Gorman, J. J., Castaldi, P. A., and Berndt, M. C. (1989) *Biochemistry 28*, 8317−8326.
9. Atoda, H., Hyuga, M., and Morita, T. (1991) *J. Biol. Chem. 266*, 14903−14911.
10. Mizuno, H., Fujimoto, Z., Koizumi, M., Kano, H., Atoda, H., and Morita, T. (1997) *Nat. Struct. Biol. 4*, 438−441.
11. Mizuno, H., Fujimoto, Z., Atoda, H., and Morita, T. (2001) *Proc. Natl. Acad. Sci. U.S.A. 98*, 7230−7234.
12. Sen, U., Vasudevan, S., Subbarao, G., McClintoch, R. A., Celikel, R., Ruggeri, Z. M., and Varughese, K. I. (2001) *Biochemistry 40*, 345−352.
13. Shelton-Inloes, B. B., Titani, K., and Sadler, J. E. (1986) *Biochemistry 25*, 3164−3171.
14. Obert, B., Houllier, A., Meyer, D., and Girma, J.-P. (1999) *Blood 93*, 1959−1968.
15. Otwinowski, Z., and Minor, W. (1997) *Methods Enzymol. 276*, 307−326.
16. Collaborative Computational Project, Number 4 (1994) *Acta Crystallogr. D50*, 760−767.
17. Brunger, A. T., Adams, P. D., Clore, G. M., DeLano, W. L., Gros, P., Grosse-Kunstleve, R. W., Jiang, J. S., Kuszewski, J., Nilges, M., Pannu, N. S., Read, R. J., Rice, L. M., Simonson, T., and Warren, G. L. (1998) *Acta Crystallogr. D54*, 905−921.
18. Laskowski, R. A., MacArthur, M. W., Moss, D. S., and Thornton, J. M. (1993) *J. Appl. Crystallogr. 26*, 283−291.
19. Kraulis, P. J. (1991) *J. Appl. Crystallogr. 24*, 946−950.
20. Nicholls, A., Sharp, K. A., and Honing, B. (1991) *Protein 11*, 281−296.
21. Matsui, T., Hamako, J., Suzuki, M., Hayashi, N., Ito, M., Makita, K., Fujimura, Y., Ozeki, Y., and Titani, K. (1997) *Res. Commun. Biochem. Cell Mol. Biol. 1*, 271−284.
22. Mizuno, H., Fujimoto, Z., Koizumi, M., Kano, H., Atoda, H., and Morita, T. (1999) *J. Mol. Biol. 289*, 103−112.
23. Bennett, M. J., Schlunegger, M. P., and Eisenberg, D. (1995) *Protein Sci. 4*, 2455−2468.
24. Atoda, H., Ishikawa, M., Mizuno, H., and Morita, T. (1998) *Biochemistry 37*, 17361−17370.
25. Shin, Y., Okuyama, I., Hasegawa, J., and Morita, T. (2000) *Thromb. Res. 99*, 239−247.
26. Fukuda, K., Mizuno, H., Atoda, H., and Morita, T. (2000) *Biochemistry 39*, 1915−1923.
27. Gernstein, M., Lesk, A. M., and Chotia, C. (1994) *Biochemistry 33*, 6739−6749.
28. Markland, F. S. (1998) *Toxicon 36* (12), 1749−1800.
29. Emsley, J., Cruz, M., Handin, R., and Liddington, R. (1998) *J. Biol. Chem. 273*, 10396−10401.
30. Matsushita, T., and Sadler, J. E. (1995) *J. Biol. Chem. 270*, 13406−13414.
31. Matsushita, T., Meyer, D., and Sadler, J. E. (2000) *J. Biol. Chem. 275*, 11044−11049.
32. Matsui, T., Matsushita, T., Saito, H., Fujimura, Y., and Titani, K. (2001) *Int. J. Hematol. 73* (Suppl.), 239.
33. Huizinga, E., Martijn, P. R., Kroon, J., Sixma, J., and Gros, P. (1997) *Structure 5*, 1147−1156.

BI0114933